Analysing the Damping of Grid-Connected Inverter by Applying Impedance-Based Sensitivity Function

1st Henrik Alenius
Faculty of Information Technology and Communication Sciences
Tampere University , Tampere, Finland
henrik.alenius@tuni.fi

2nd Tomi Roinila
Faculty of Information Technology and Communication Sciences
Tampere University , Tampere, Finland
tomi.roinila@tuni.fi

***Abstract*—Stability issues have emerged in the grid interfaces of power electronics when the grid impedance is high or multiple devices are connected in parallel. Impedance-based stability criterion has demonstrated high applicability in the stability assessment, as the analysis can be performed based on the terminal impedances of the grid and the converter. Typically, impedance measurements are required to obtain the terminal impedances. However, extracting the stability margins and predicting the system dynamics from the measured impedances typically requires complex methods, such as transfer function fitting. This work proposes an extension to the impedance-based stability criterion, where the critical system damping and the critical resonant mode are extracted from the impedance data. An impedance-based sensitivity function is constructed from the terminal impedances, and the system damping factor is calculated from the sensitivity function. A second-order transfer function is constructed from the obtained damping factor and resonant frequency, which captures the critical resonant mode of the system. The method is validated in experimental stability analysis of a 2.7 kW grid-connected three-phase inverter, where the method accurately predicts the resonant dynamics of the system when the stability margins are low.**

***Index Terms*—Stability analysis, Sensitivity function, Impedance-based stability criterion, Impedance measurements.**

I. Introduction

The rapid increase in the amount of grid-connected power electronics has disrupted the dynamics of modern power systems and exposed challenges in the control and stability of the system. The interactions of power-electronic devices in the grid interface have been shown to expose the system to instability [1]–[5]. To predict the stability issues, impedance-based stability analysis has been proposed. In the method, the interface stability is assessed through impedances of both subsystems [6].

This work extends the conventional impedance-based stability criterion by proposing a straightforward method for predicting the critical system dynamics and resonant modes from the impedance measurements. In the method, the system damping factor and critical frequency are obtained from the impedance-based sensitivity function. Then, a second-order transfer function estimate is constructed from the damping factor and frequency, which accurately captures the critical resonant mode of the system. As a result, the system stability margins and transient dynamics can be predicted. The performance of the proposed method is verified through stability analysis of a grid-connected three-phase inverter. The q-components of the inverter output admittance and the grid impedance are measured, and the presented method is applied. The obtained estimate is shown to accurately predict the system robustness and stability margins.

Performing the impedance-based analysis requires the terminal impedances of the subsystems. However, the detailed structure of a power system is often unknown due to very high number of electronic devices and high system complexity. Additionally, the precise internal dynamics of commercial devices are often protected by the manufacturer. Consequently, measurements have been widely applied to obtain the terminal impedances of systems [2]–[5], [7], [8].

Recently, broadband excitation sequences have been applied in the impedance measurements, as they exhibit multiple desirable characteristics, such as fast measurement duration, controllable frequency bandwidth and resolution, low crest factor, and they are easy to generate [8]–[13]. One of the most widely applied broadband sequence is the maximum-length binary sequence (MLBS). However, the MLBS suffers from very limited number of available signal lengths, which are available for $N = 2^n - 1$, where n is a positive integer. Therefore, the signal length is approximately doubled each time when a signal of higher length is required. This may cause issues in practical implementations which are often characterized by tight constraints in computing power.

As a second contribution, this work applies a quadratic-residue binary sequence (QRBS), originally introduced in [14], in the impedance measurements of a power electric system. The QRBS has similar favorable characteristics than the MLBS, but the sequence length has drastically more options as the sequence is available for lengths $N = 4k - 1$, where k is a positive integer and N is a prime.

The remainder of the work is organized as follows. Section II reviews the theoretical background of the impedance-based stability analysis. Section III discusses the impedance measurements and presents the quadratic-residue binary sequence (QRBS). In Section IV, the proposed method for estimating the critical system dynamics is presented. Section V shows the experimental measurements and validation of the presented method. Finally, Section VI concludes the work.

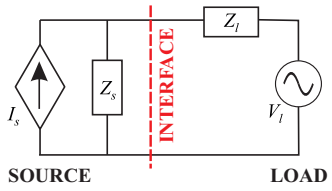

Fig. 1. Source-load equivalent of interconnected subsystems

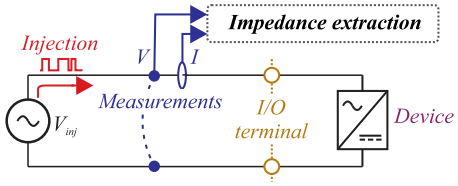

Fig. 2. Simplified diagram of an impedance measurement.

II. Impedance-based stability analysis

Fig. 1 shows the equivalent circuit for the system, where a grid-connected inverter is modeled as a Norton equivalent and the grid as a Thevenin equivalent. The stability of the interconnected subsystems can be assessed directly from the impedance-based characteristic equation

$$C(s) = \frac{1}{1 + Y_{\mathrm{o}}(s)Z_{\mathrm{g}}(s)} = \frac{1}{1 + Z_{\mathrm{g}}(s)/Z_{\mathrm{o}}(s)} \tag{1}$$

where $Y_{\mathrm{o}}(s) = 1/Z_{\mathrm{o}}(s)$ is the output admittance of the power-electronic device $Z_{\mathrm{g}}(s)$ is the grid impedance [6]. The stability analysis can be performed by applying Nyquist criterion to the impedance ratio $Z_{\mathrm{g}}(s)/Z_{\mathrm{o}}(s)$.

A. DQ-Domain Impedance

Power-electric devices are often controlled in the dq-domain, where the three AC signals of a three-phase system can be reduced to two DC valued signals through Park's transformation [15]. Consequently, the impedance measurements are often performed in the same dq-frame to allow straightforward analysis. The direct components (d and q) are coupled through crosscouplings (dq and qd) and the system impedance (admittance) is defined as

$$\begin{bmatrix} V_{\mathrm{d}}(s) \\ V_{\mathrm{q}}(s) \end{bmatrix} = \begin{bmatrix} Z_{\mathrm{dd}}(s) & Z_{\mathrm{qd}}(s) \\ Z_{\mathrm{dq}}(s) & Z_{\mathrm{qq}}(s) \end{bmatrix} \begin{bmatrix} I_{\mathrm{d}}(s) \\ I_{\mathrm{q}}(s) \end{bmatrix} \tag{2}$$

where V is the voltage, Z is the impedance, I is the current, and the subscripts indicate the component in the dq-domain.

In the dq-domain analysis, accurate stability assessment requires the use of multivariable models, where both the d- and q-components, as well as crosscouplings, are taken into account. Thus, the impedances become 2x2-matrices and the stability analysis must be performed by applying the generalized Nyquist criterion (GNC), where two eigenvalue contours are drawn in the complex plane [16], [17]. However, in grid-feeding inverters the origin of the stability issues is often the phase-locked loop which affects the qq-component of the impedance [18]. Therefore, without significant loss of accuracy, the stability analysis can be performed by assessing the qq-components of the grid impedance and inverter output admittance.

B. Sensitivity Function

The stability analysis based on Nyquist contour shows the absolute stability of the system. However, the stability margins of the system are typically as important as the absolute stability. For stable systems, the stability margins can be deduced from the distance from the Nyquist contour to the critical point. To quantify the stability margins, impedance-based sensitivity function has been applied [19], which shows the frequency-dependent distance of the contour to the critical point. The sensitivity function can be given as

$$S(\omega) = |1/\big(1 + Y_{\mathrm{o}}(\omega)Z_{\mathrm{g}}(\omega)\big)| \tag{3}$$

where $Y_{\mathrm{o}}(\omega)$ is the output admittance of the inverter and $Z_{\mathrm{g}}(\omega)$ is the grid impedance. The sensitivity peak is defined as $M_{\mathrm{s}} = \max(S)$, where the peak occurs at the critical frequency ω_{c}.

III. Perturbation Design

To facilitate the use of impedance-based stability criterion, methods for measuring the terminal impedance have been presented [2], [7], [8]. Typically, the impedance measurements are performed by injecting a perturbation signal to the system, measuring the voltages and currents, and obtaining the frequency-response through Fourier techniques. The perturbation is injected to the system as a voltage- or current-type excitation, for example by applying the current references of an inverter or grid voltage references. Fig. 2 shows a simplified diagram of a terminal impedance measurement of a grid-connected device.

A. Broadband Perturbations

Recently, broadband sequences have shown many desirable characteristics for impedance measurements, and especially maximum-length binary sequence (MLBS), originally introduced in [20], has been widely adopted [7], [11], [21], [22]. The MLBS is a pediodic and deterministic binary sequence that has a length of N and is generated at f_{gen}. The frequency spectrum is linearly spaced with a resolution of $f_{\mathrm{res}} = f_{\mathrm{gen}}/N$, and the measurement duration of a period is $T_{\mathrm{meas}} = 1/f_{\mathrm{res}}$.

B. Quadratic-residue binary sequence

Quadratic-residue binary sequence (QRBS) is a form of periodic pseudo-random signal originally introduced in [14]. The QRBS has the following properties:

1) the length of the signal can be chosen as $N = 4k - 1$
2) the signal alternates between two levels with almost uniform distribution between the levels
3) the signal value can change only at discrete times every $1/f_{\mathrm{gen}}$
4) the signal is deterministic, allowing repeatable experiments
5) the signal is periodic over $t_{\mathrm{m}} = N/f_{\mathrm{gen}}$, allowing averaging over multiple periods

where N is a prime number, k is a positive integer, f_{gen} is the generation frequency, and t_{m} the duration of one period [12].

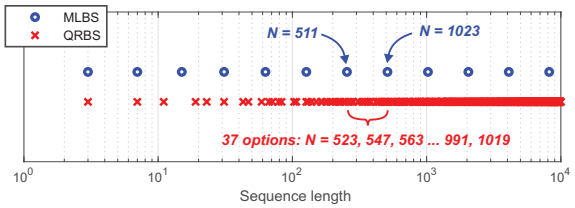

Fig. 3. Available signal lengths for MLBS (blue) and QRBS (red).

The characteristics of the QRBS are similar to the MLBS, but a significant difference is found from the available signal lengths. As the MLBS is available only for $N = 2^n - 1$, where n is a positive integer, it is apparent that the length of the QRBS has drastically more options. Fig. 3 presents the available signal lengths for both the MLBS and QRBS up to 10000.

The design of the QRBS is well documented [12], and can be summarized as follows

1) Choose a signal length of $N = 4k - 1$, where N is a prime and k a positive integer
2) Form a sequence up to $(N-1)/2$, $[1\ 2\ ...\ (N-1)/2]$
3) Square the sequence, $[1^2\ 2^2\ ...\ ((N-1)/2)^2]$
4) Take mod-N of all the values, $[1_{modN}\ 2_{modN}\ ...\ ((N-1)/2)_{modN}]$
5) Generate a sequence of zeros with a length of N
6) Set the values in empty sequence to one based on the modulo sequence (that is, if the modulo sequence in (4) contains a number 1, the 1st element of the sequence full of zeros is replaced by one).
7) From the obtained sequence, map values of 0 to -1.

A design example for QRBS that has $N = 7$ is presented in the Appendix A.

IV. System Damping Factor Estimation

In this work, the impedance-based stability criterion is extended by extracting the system damping and resonant frequency from the impedance data through the use of the impedance-based sensitivity function. Fig. 4 presents the method this work proposes for extending the impedance-based stability criterion. The steps of the method are as follows

1) Measure the terminal impedances, $Y_{\text{o-qq}}$ and $Z_{\text{g-qq}}$
2) Calculate the sensitivity function S
3) Obtain the corresponding minimum phase margin Φ_m from the sensitivity function
4) Calculate the damping factor ζ from the Φ_m
5) Extract the critical frequency ω_c from the peak value of the sensitivity function
6) Calculate the natural resonant frequency ω_n
7) Formulate a second-order estimate from ζ and ω_n.

The minimum phase margin can be defined from the sensitivity function peak by applying

$$\Phi_\text{m} = 2 * \text{asin}\left(\frac{1}{2M_\text{s}}\right) \tag{4}$$

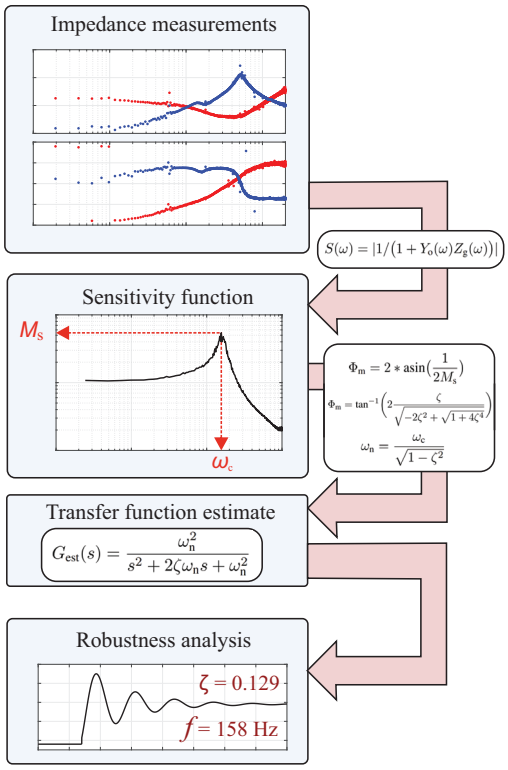

Fig. 4. Flowchart of the proposed method.

where M_s is the sensitivity peak (maximum of the sensitivity function). Additionally, the phase margin and damping factor are related through

$$\Phi_\text{m} = \tan^{-1}\left(2\frac{\zeta}{\sqrt{-2\zeta^2 + \sqrt{1+4\zeta^4}}}\right) \tag{5}$$

which can be simplified as $\zeta \approx 0.01\Phi_\text{m}$ for low values of damping factor. Moreover, the critical resonant frequency ω_c can be directly obtained from the frequency of the sensitivity function maximum. The natural resonant frequency of the system can be given as

$$\omega_\text{n} = \frac{\omega_\text{c}}{\sqrt{1-\zeta^2}} \tag{6}$$

Finally, when the damping factor and frequency are known, a second-order transfer function can be build to approximate the critical system dynamics given as

$$G_\text{est}(s) = \frac{\omega_\text{n}^2}{s^2 + 2\zeta\omega_\text{n}s + \omega_\text{n}^2} \tag{7}$$

This transfer function can be directly used to approximate the system dynamics based on the critical frequency. In system that has low stability margins, the transfer function shows the shape of the transient response. Additionally, the damping factor can be used as a quantitative measure for system robustness, and the critical frequency can be utilized in the system design to strengthen the system by, for example, controller re-design.

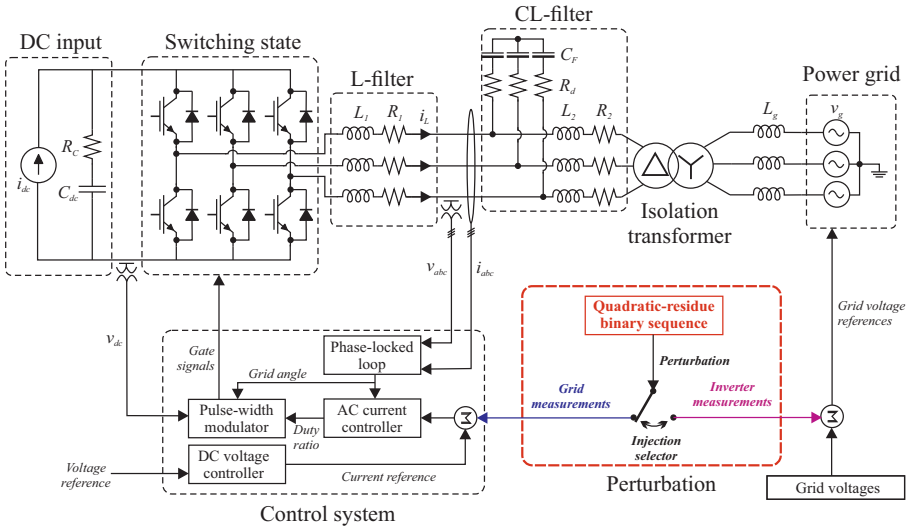

Fig. 5. Experimental setup configuration.

V. Experiments

The performance of the proposed method is verified with an experimental setup that consists of a 2.7 kW three-phase inverter (*Myway Plus MWINV-9R144*), a linear voltage amplifier (*Spitzenberger & Spies PAC 15000*), and a PV emulator (*Spitzenberger & Spies PVS 7000*). Fig. 5 presents the detailed configuration of the experimental setup. The controller of the inverter is implemented in a dSPACE real-time simulation. The inverter has an L-filter, and is interfaced to the grid (voltage amplifier) through an external CL-filter, an isolation transformer, and an additional inductor that emulates the grid impedance. The system parameters are shown in Table II in Appendix B.

A. Impedance measurements

In this work, the stability analysis is performed based on the q-channel impedances of the interconnected inverter and grid. First, the inverter output admittance is measured by injecting a broadband perturbance to the grid voltages and obtaining the admittance through Fourier methods. Then, an additional inductor is connected to the system to emulate the grid impedance, and the grid impedance is measured by performing the perturbation injection through the current reference of the inverter. The parameters of the QRBS perturbation are shown in Table I. Fig. 6 presents the measurement configuration for (a) grid impedance measurements and (b) inverter admittance measurements. Fig. 7 shows the measured grid impedance q-component and Fig. 8 shows the inverter output admittance q-component.

TABLE I
Perturbation parameters for measurements.

Parameter	Value	Parameter	Value
Sequence length	1999	Generation frequency	8 kHz
Average periods	50	Frequency resolution	2.0 Hz
Amplitude (V-type)	3 V	Amplitude (I-type)	0.2 A

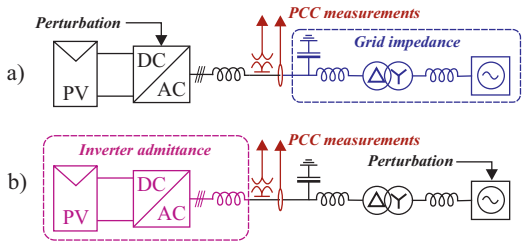

Fig. 6. Measurement configuration for (a) grid impedance and (b) inverter admittance measurements.

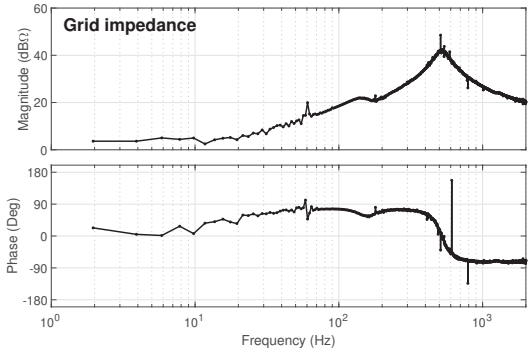

Fig. 7. Measured grid impedance q-component.

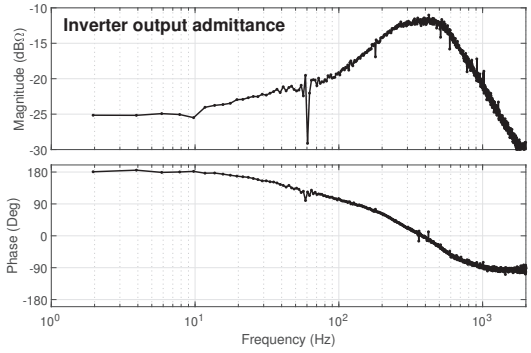

Fig. 8. Measured inverter output admittance q-component.

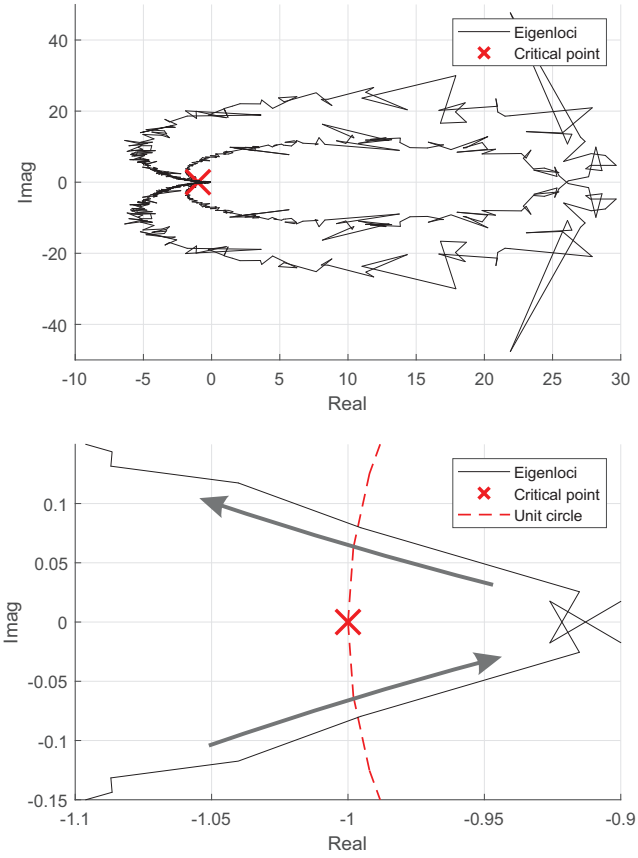

Fig. 9. Nyquist contour of the impedance ratio (upper) and zoomed contour around critical point (lower).

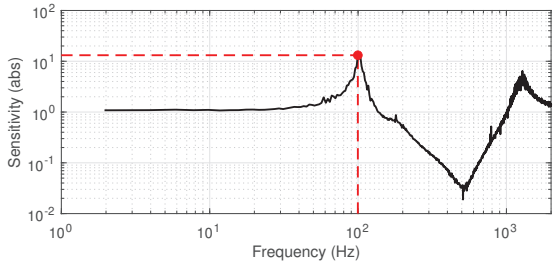

Fig. 10. Impedance-based sensitivity function (sensitivity peak indicated with red).

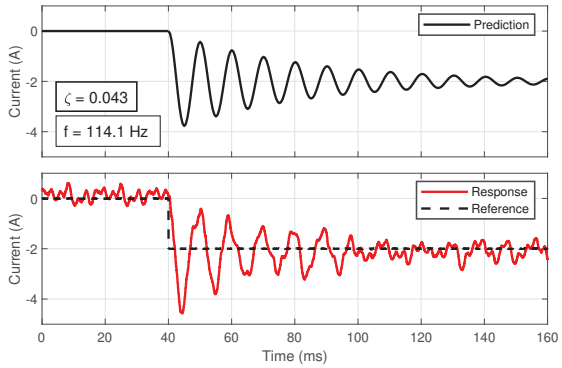

Fig. 11. Predicted dynamic performance (black) and actual system response (red).

B. Stability analysis

The stability analysis is performed based on the measured impedances by applying Nyquist criterion and the proposed method. Fig. 9 shows the Nyquist contour (eigenlocus) which is calculated from the impedance ratio. The contour does not encircle the critical point, which indicates stable operation. However, the contour passes close to the critical point, which suggests the possibility of low stability margins.

To assess the stability margins quantitatively, the proposed method is applied. First, the impedance-based sensitivity function shown in Fig. 10 is calculated by applying (3). From the sensitivity function, the peak can be identified to have a magnitude of $M_s = 13.1$ and an angular frequency of $\omega_c = 626.2$ rad/s. Next, the minimum phase margin and corresponding damping factor are calculated by applying (4) and (5), which yield $\Phi_m = 4.36$ degrees and $\zeta = 0.0381$. Applying (6), the natural resonant frequency is ω_n. Finally, the second-order estimate of the system can be calculated from (7), yielding

$$G_{est}(s) = \frac{392700}{s^2 + 47.71s + 392700} \tag{8}$$

The obtained transfer function can be applied to predict the system transient responses, where the damping factor gives a quantitative value for the system robustness. To verify the prediction, the operation of the system is disturbed with a step change of q-channel current reference. Fig. 11 presents the predicted current response to the reference change (black, upper) and the measured step response (red, lower). Ideally, the current should follow the reference closely and have a similar shape. However, due to the low stability margins resulting from the high-impedance grid, the system damping factor is low and the response is highly resonant. As seen from the figure, the second-order estimation that was obtained by applying the proposed method gives an accurate prediction of the response, and thus, describes the system damping factor. The estimation indicates slightly lower damping factor compared to the actual value. This can be explained by examining Equation (4). The equation yields the minimum phase margin, so the actual phase margin of the system can be slightly higher. However, the error is negligible and always in the manner where a worst-case robustness is predicted. Therefore, the method can be considered to ensure the stability with a safety factor.

VI. Conclusion

The impedance-based stability criterion has become a widely applied method for stability analysis of grid-connected systems. This work has extended the stability criterion, and presented a method for quantifying quantifying the stability margins obtained through the impedance measurements. In

addition, in order to improve the conventional impedance-measurement technique based on the maximum-length binary sequence (MLBS), the quadratic-residue binary sequence (QRBS) was applied. Compared to the MLBS, the QRBS has a significantly higher number of available signal lengths, thus making it possible to more efficiently optimize the practical measurement setup. The method was shown to accurately capture the damping factor and to predict the system responses to transients in experimental system of a grid-connected inverter.

Appendix A: Generating 7-bit-long QRBS

This appendix shown the design of 7-bit-long QRBS as an example, where the steps are

1) $N = 4k - 1 = 7$, where $k = 2$ and N is prime
2) Form basic sequence: [1 2 3]
3) Square the sequence: [1 4 9]
4) Take mod-7 of the sequence: [1 4 2]
5) Generate zero sequence: [0 0 0 0 0 0 0]
6) Set 1st, 2nd, and 4th bit to 1: [1 1 0 1 0 0 0]
7) Map zeros to -1: [1 1 -1 1 -1 -1 -1].

Similarly, sequences with different lengths can be designed for $N = 4k - 1$, where N is a prime number and k is a positive integer.

Appendix B: System Parameters

TABLE II
Parameters of the experimental setup.

Parameter	Symbol	Value
Grid frequency	f_{n}	60 Hz
Grid phase voltage	V_{g}	120 V
Inverter nominal power	S_{n}	2.7 kVA
Switching frequency	f_{sw}	8 kHz
Power factor	$\cos\phi$	1.0
Switching deadtime	T_{dt}	4.0 μs
DC voltage	V_{dc}	414.3 V
DC input current	I_{dc}	6.577 A
DC capacitor capacitance	C_{dc}	1.5 mF
L-filter inductance	L_1	2.2 mH
L-filter resistance	R_1	100 mΩ
CL-filter inductance	L_2	0.6 mH
CL-filter resistance	R_2	100 mΩ
CL-filter capacitance	C_{f}	10 μF
CL-filter damping resistance	R_{d}	1.8 Ω
Transformer inductance	L_{tf}	0.3 mH
Transformer resistance	R_{tf}	400 mΩ
Grid inductance	L_{g}	9 mH
AC current control proportional gain	$K_{\text{P-CC}}$	0.0149
AC current control integral gain	$K_{\text{I-CC}}$	23.442
DC voltage control proportional gain	$K_{\text{P-VC}}$	0.0962
DC voltage control integral gain	$K_{\text{I-VC}}$	1.2092
PLL control proportional gain	$K_{\text{P-PLL}}$	2.3280
PLL control integral gain	$K_{\text{I-PLL}}$	351.720

References

[1] C. Li, "Unstable Operation of Photovoltaic Inverter from Field Experiences," *IEEE Transactions on Power Delivery*, vol. 8977, no. c, pp. 1–1, 2017.

[2] Y. Tang, R. Burgos, B. Wen, D. Boroyevich, J. Verhulst, D. Vrtachnik, and M. Belkhayat, "A Novel dq impedance measurement method in three-phase balanced systems," in *2019 IEEE 20th Workshop on Control and Modeling for Power Electronics, COMPEL 2019*, 2019.

[3] T. Roinila, T. Messo, and E. Santi, "MIMO-identification techniques for rapid impedance-based stability assessment of three-phase systems in DQ Domain," *IEEE Transactions on Power Electronics*, vol. 33, no. 5, pp. 4015–4022, 2018.

[4] T. Suntio, T. Messo, M. Berg, H. Alenius, T. Reinikka, R. Luhtala, and K. Zenger, "Impedance-Based Interactions in Grid-Tied Three-Phase Inverters in Renewable Energy Applications," *Energies*, vol. 12, no. 464, 2019.

[5] H. Alenius and T. Roinila, "Impedance-Based Stability Analysis of Paralleled Grid-Connected Rectifiers: Experimental Case Study in a Data Center," *Energies*, vol. 13, no. 2109, 2020.

[6] J. Sun, "Impedance-based stability criterion for grid-connected inverters," *IEEE Transactions on Power Electronics*, vol. 26, no. 11, pp. 3075–3078, 2011.

[7] R. Luhtala, T. Roinila, and T. Messo, "Implementation of Real-Time Impedance-Based Stability Assessment of Grid-Connected Systems Using MIMO-Identification Techniques," *IEEE Transactions on Industry Applications*, vol. 54, no. 5, pp. 5054–5063, 2018.

[8] A. Riccobono, M. Cupelli, A. Monti, E. Santi, T. Roinila, H. Abdollahi, S. Arrua, and R. A. Dougal, "Stability of shipboard dc power distribution: Online impedance-based systems methods," *IEEE Electrification Magazine*, vol. 5, no. 3, pp. 55–67, 2017.

[9] R. Luhtala, H. Alenius, T. Messo, and T. Roinila, "Online Frequency Response Measurements of Grid-Connected Systems in Presence of Grid Harmonics and Unbalance," *IEEE Transactions on Power Electronics*, vol. 35, no. 4, pp. 3343–3347, 2020.

[10] T. Roinila and T. Messo, "Online Grid-Impedance Measurement Using Ternary-Sequence Injection," *IEEE Transactions on Industry Applications*, vol. 54, no. 5, pp. 5097–5103, 2018.

[11] T. Roinila, T. Messo, T. Suntio, and M. Vilkko, "Pseudo-Random Sequences in DQ-Domain Analysis of Feedforward Control in Grid-Connected Inverters," *IFAC-PapersOnLine*, vol. 48, no. 28, pp. 1301–1306, 2015.

[12] A. H. Tan and K. Godfrey, *Industrial Process Identification - Perturbation Signal Design and Applications*, 1st ed. Springer, 2019.

[13] H. Alenius, T. Roinila, R. Luhtala, T. Messo, A. Burstein, E. de Jong, and A. Fabian, "Hardware-in-the-Loop Methods for Stability Analysis of Multiple Parallel Inverters in Three-Phase AC Systems," *IEEE Journal of Emerging and Selected Topics in Power Electronics*, pp. 1–10, 2020. [Online]. Available: https://dx.doi.org/10.1109/JESTPE.2020.3014665

[14] D. Everett, "Periodic digital sequences with pseudonoise properties," *G.E.C Journal*, vol. 33, no. 115-126, 1966.

[15] T. Suntio, T. Messo, and J. Puukko, *Power Electronics Converters - Dynamics and Control in Conventional and Renewable Energy Applications*. Wiley-VCH, 2017.

[16] M. Belkhayat, "Stability criteria for AC power systems with regulated loads," Doctoral thesis, Purdue University, 1997.

[17] A. G. J. Macfarlane and I. Postlethwaite, "The generalized nyquist stability criterion and multivariable root loci," *International Journal of Control*, vol. 25, no. 1, pp. 81–127, 1977.

[18] T. Messo, J. Jokipii, A. Mäkinen, and T. Suntio, "Modeling the grid synchronization induced negative-resistor-like behavior in the output impedance of a three-phase photovoltaic inverter," *2013 4th IEEE International Symposium on Power Electronics for Distributed Generation Systems, PEDG 2013 - Conference Proceedings*, pp. 1–7, 2013.

[19] S. Vesti, T. Suntio, J. A. Oliver, R. Prieto, and J. A. Cobos, "Impedance-based stability and transient-performance assessment applying maximum peak criteria," *IEEE Transactions on Power Electronics*, vol. 28, no. 5, pp. 2099–2104, 2013.

[20] W. Davies, "Using the binary maximum length sequence for the identification of system dynamics," *Proceedings of the Institution of Electrical Engineers*, vol. 114, no. 10, p. 1582, 1967.

[21] T. Messo, R. Luhtala, A. Aapro, and T. Roinila, "Accurate Impedance Model of Grid-Connected Inverter for Small-Signal Stability Assessment in High-Impedance Grids," in *2018 International Power Electronics Conference*, no. 1, 2018, pp. 3156–3163.

[22] Y. Han, M. Yang, H. Li, P. Yang, L. Xu, E. A. A. Coelho, and J. M. Guerrero, "Modeling and Stability Analysis of LCL-Type Grid-Connected Inverters: A Comprehensive Overview," *IEEE Access*, vol. 7, pp. 114 975–115 001, 2019.